Theoretical Study on the Size and the Shape of Linear Dendronized Polymers in Good and Selective Solvents

Pavlos Efthymiopoulos, Costas Vlahos, and Marios Kosmas*

Department of Chemistry, University of Ioannina, 45110 Ioannina, Greece

Received July 17, 2008; Revised Manuscript Received December 3, 2008

ABSTRACT: The conformational properties of linear dendronized polymers made of a backbone and grafted dendrons are studied analytically as a function of the molecular weights of the backbone and the dendrons. Our previous model for dendritic homopolymers with a central core, is extended to include dendritic structures emerging from a linear polymeric chain made of units of different chemical nature. The ways the number of dendrons, their generation, and the functionality of their branching points affect the size and the shape both of the backbone and the dendrons are given in detail. The various effects of the quality of the solvent, capable to be different for the dendrons and the backbone, lead to interesting novel behaviors.

1. Introduction

The large degree of vacancies in the interior of dendritic polymers offer them the ability to encapsulate and release guest molecules which makes them successful delivery vehicles both for drugs but also for other cargos.[1] Their numerous end groups with the capability to be connected to various chemical functionalities at spatially defined locations with a varying degree of accessibility make them find applications in fields like catalysis[2] or solubility.[3] The interesting properties of dendritic polymers can even be better in more complex structures coming from the connection of dendritic polymers with a linear macromolecular chain. Such systems are the linear dendronized polymers[4] (LDPs) which are composed of many grafted dendrons emerging at regular intervals on the backbone chain, Figure 1.

The presence of the polymeric backbone can support larger structures enriching the central spherical structures which the dendritic polymers can have. The total molecular weight M of a LDP is equal to:

$$M = M_b + (n+1)M_d = n \times N_b + (n+1)\frac{(f-1)^{g+1}-1}{f-2}N_d \quad (1)$$

where M_b and M_d, are the molecular weights of the backbone and of each grafted dendron, while N_b and N_d are the molecular weights of a backbone segment and of a dendron's branch respectively. The total number of backbone segments is n, f is the dendron's branching point functionality and g the dendron's number of generations. Structures from disk-like and spherical to more elongated shapes and rods are possible by changing microscopic parameters like the number of generations g,[5−7] the quality of the solvent[5] or the degree of polymerization of the dendrons or the backbone.[5,8−10] This possibility to form objects with controllable dimensions, shape, structure, and chemical functionality on the nanometric scale makes them challenging in the area of nanotechnology useful for example as building blocks in the manufacture of nanomaterials. An open challenge is the determination of the way which various parameters affect the conformations of the backbone and the dendrons and thus the size and the shape of these macromolecules. Beyond the molecular weights of the dendrons and the backbone, the functionality f of the branching points, the number g of the generations of dendrons and the grafting density of dendrons, the quality of solvent is another parameter which plays an important role in the determination of the macroscopic behavior. In the limit of large grafting densities, the many interactive dendrons not only increase the stiffness of the backbone of dendronized polymers but also bring signs of organized helical arrangements of their dendrons. Such local structures have been detected both by NMR spectroscopy[11] and theoretical calculations.[12] Larger backbones though, with smaller numbers of dendrons are more flexible leading to disordered structures leaving only global features to characterize dendronized polymers. This last region is the one we intend to study, aiming to give in detail the effects which the microscopic parameters cause on the size and shape of dendronized polymers made of a backbone and grafted dendrons built generally from different monomeric units.

Previous studies of the cases of flexible dendronized polymers include experimental and computational efforts for the determinations of the regularities of the size and shape of their chains. Their encapsulation properties, like those of simpler dendritic polymers,[13] have been shown by means of NMR to increase with the number of generations[14] indicating an enlargement of the number of vacancies in their interior. Viscosity measurements[5,15] and SEC techniques[16] have been employed for the study of the transition from spherical to extended structures where the size of the backbone was found to increase slowly when the number of generations g is small and more rapidly when g is large. The transition from flexible and coil-like to rod-like as the g increases has also been studied by means of SANS[6] and the radius of gyration[17] and the average diameter of dendronized polystyrenes were found to increase almost linearly with g for small g.[18] By means of light scattering techniques the radius of gyration was also found to increase with g.[7,15]From the theoretical point of view the dendron size was found to increase almost linearly with g[19] and Monte Carlo[20] as well as Brownian dynamics simulations[10] gave that the elongation of the backbone is increasing on increasing the length of the branch of the dendrons N_d, their generations g, or the dendron grafting density. Of interest is the observation that the quality of the solvent plays an important role to the transition from the spherical to an extended (cylindrical) structure.[5] By means of SANS[17] and NMR[21] the size of dendronized polymers was also found to increase with solvent's quality. The interest is that the usual dendronized polymers are actually branched copolymers with dendrons and backbones made of different species. These two parts of the polymer can have different conformational properties depending on the quality of the solvent which depends on the nature of the monomeric units

* Corresponding author. E-mail: mkosmas@cc.uoi.gr.

10.1021/ma801609f CCC: $40.75
Published on Web 01/21/2009

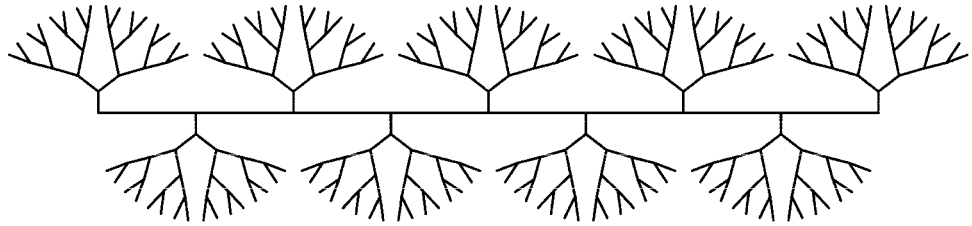

Figure 1. Schematic representation of a LDP with $n = 8$ backbone segments, $g = 4$ generations of the dendrons and functionality of the branching points $f = 3$.

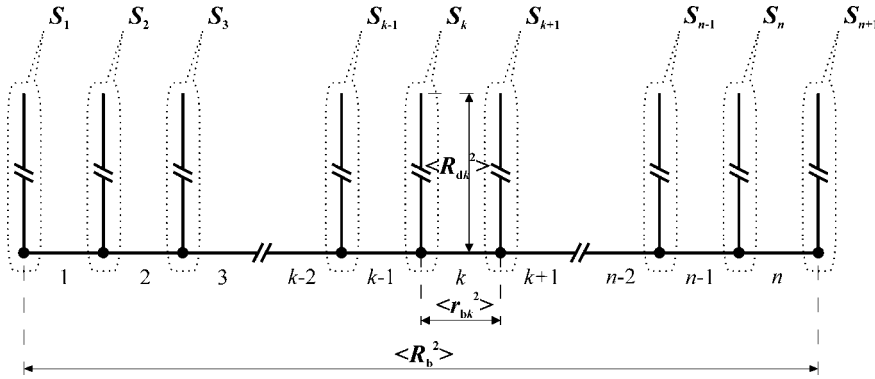

Figure 2. Two-dimensional image of a LDP. The horizontial line represents the backbone, while the perpendicular lines represent the grafted dendrons.

that of the solvent but also temperature. They can even have opposite behavior on the same chain leading to new overall features which can easily be changed by changing the solvent, the nature of monomers or the temperature. This is one of our main interest in undertaking the study of these polymers. We aim also in determining in quantitative detail the transition to extended or shrink structures as a function of the "topological" characteristics of these giant molecules.

2. The Model

The dendronized polymers which we study are copolymers and include $n+1$ dendrons of the same species, connected with n segments of length N_b each made of a second different species forming so the backbone of the dendronized polymer of length $n \times N_b$, Figure 2. Each dendron has branches of length N_d, a branching functionality f and a generation number g and it is connected with the backbone with a branch of length N_d. We denote with $k = 1, 2, ..., n$ the backbone spacers of length N_b between the n grafting points. Each of the n identical dendrons starts with a branch and grows up to g generations and consists of $((f-1)^{g+1} - 1)/(f-2)$ branches of length N_d. Following our previous work,[22] we write for the probability distribution function of the dendronized polymer with interacting branching points the expression:

$$P[R(s)] = P_0[R(s)] \exp\Big[-u_{dd}\sum_{d}\sum_{d'}\delta(R_d - R_{d'}) - u_{db}\sum_{d}\sum_{b}\delta(R_d - R_b) - u_{bb}\sum_{b}\sum_{b'}\delta(R_b - R_{b'})\Big] \quad (2)$$

Here $P_0[R(s)]$ is the ideal connectivity term of the dendronized polymer of the Gaussian type while the R's in the exponent of eq 2 stand for the positions of all interacting branching points. The R_d, $R_{d'}$ describe the positions of branching points of the dendrons while the R_b, $R_{b'}$ describe those on the backbone. δ is the 3-dimensional Dirac delta function which brings in contact all pairs of interacting points of the macromolecule. Three interaction parameters u_{dd}, u_{bb}, and u_{db} are used to describe the intensity of the interactions between two dendron, two backbone, and one dendron and one backbone branching points respectively, which as in the initial Fixmann−Edwards model are proportional to the binary cluster integrals.[23,24] Positive and negative values of u's mean repulsions (good solvent) and attractions (poor solvent) respectively, while the value zero represents the Θ solvent conditions. The mean end-to-end square distances of the various parts of the dendronized polymer are obtained from expressions of the form

$$\langle R^2 \rangle = \frac{\int D[r(s)]R^2 P[r(s)]}{\int D[r(s)]P[r(s)]} \quad (3)$$

where $D[r(s)]$ is the measure of the path integrals, which expresses the integrations over all points of the chain in the continuous line limit. Expanding eq 2 in increasing powers of the three interaction parameters u and taking into account that δ functions bring in contact branching points we obtain, by means of eq 3, the following general expression for the mean end-to-end square distances up to first order in the u parameters:

$$\langle R^2 \rangle = \langle R^2 \rangle_0 [1 + N_b^{-3/2}(u_{dd}C_{dd} + u_{db}C_{db} + u_{bb}C_{bb}) + O(N_b^{-3}u^2)] \quad (4)$$

where $\langle R^2 \rangle_0$ is the ideal chain result of the corresponding part of the macromolecule and the O part represent terms of second or higher order in the parameters $N_b^{-3/2}u_{ij}$. For simplicity the Kuhn lengths of the backbone's and dendron's polymeric chains are taken equal to one leaving N_b and N_d to characterize the different molecular weights of the backbone and dendron spacers. The c_{ij} functions of the first order term depend on the topological parameters of the dendronized polymer n, g, f and the ratio $\rho = N_d/N_b$ of the two lengths. It is easily seen from eq 4 that for large molecular weights N_b of the spacers the first order term is a small quantity, much smaller than that of the full excluded volume problem which goes as $N_b^{1/2}$.[25] Though the $N_b^{-3/2}$ term decreases with N_b it is certainly much larger

than the higher order terms being of $N_b^{-3m/2}$ order. Thus we can describe properly the conformational properties of the dendronized polymers in the limit of large molecular weights by means of a first-order perturbation theory, by taking into account both the dendritic and the linear chain nature of these molecules. A thing to mention is that this first order result can be used in re-exponentiation techniques to include higher order contributions as well which do not change the main tendencies of the conformational properties. However, the values of N_b and N_d are chosen in the present effort so that the second order terms are smaller than the first order ones and the expansion factors remain smaller than 2. With these values of the segment's molecular weights no higher order terms or three body interactions are necessary to describe the conformational properties neither in the good nor in the beginning bad solvent conditions. The analytical evaluation of the first order result linear in the three interaction parameters u which includes the contribution from all loops is not trivial. We know from previous works[26] that the first order contribution to the mean end-to-end square distance from a loop, of length Nl, and probability $(3/(2\pi Nl^2))^{3/2}$ in any polymer structure is $u(3/(2\pi l^2))^{3/2}C_m{}^2/N^{5/2}$, where u can be any of the three interaction parameters u_{dd}, u_{bb}, and u_{db} and l is the Kuhn length. C_m is the length of the common part between the segment and the loop and it is easily seen from this expression that if there is no common part between the segment and the loop the corresponding diagram vanishes. For simplicity the constant $(3/(2\pi l^2))^{3/2}$ of dimension length^{-3} can be absorbed into the interaction parameters u which having initially dimensions of length^3 become dimensionless. Taking into account that the loop length N is also dimensionless we see that the dimensions of the first order perturbation terms are those of $C_m{}^2$ proportional to l^2 as expected. This leads to the equations 5 to 7 given below.

In order to be able to express all nonzero interactions between pairs of branching points we assort the interacting points into groups denoted by the symbols S_1, S_2,..., S_{n+1} shown in Figure 2. Each group consists of two subgroups, ${}^dS_k$ and ${}^bS_k$, which represent the kth dendron's branching points and the kth grafting point along the backbone respectively. The interactions between the ith and jth groups of branching points are denoted as $S_i \times S_j$. By expressing the contribution of various pairs of interacting branching points with multiple summations, the mean square end-to-end distance of the backbone, $\langle R_b{}^2\rangle$ (Figure 2), can be expressed as follows:

$$\langle R_b{}^2\rangle = N_b\left(n + \frac{2}{N_b{}^{3/2}}(u_{bb}A + u_{db}B + u_{dd}C)\right), \quad n = 1, 2, \ ...$$

where

$$A = {}^bS_{1\le i\le n+1}\times {}^bS_{1\le j<i} = \sum_{i=1}^{n}\sum_{j=1}^{i} j^{-1/2}$$

$$B = {}^bS_{1\le i\le n+1}\times {}^dS_{1\le j\le n+1}(i\neq j) = 2\sum_{i=1}^{n}\sum_{j=1}^{i}\sum_{j'=0}^{g}\frac{(f-1)^{j'}j^2}{(j+(j'+1)\rho)^{5/2}}$$

$$C = {}^dS_{1\le i\le n+1}\times {}^dS_{1\le j<i} = \sum_{i=1}^{n}\sum_{j=1}^{i}\sum_{i'=0}^{g}\sum_{j'=0}^{g}\frac{(f-1)^{i'+j'}j^2}{(j+(i'+j'+2)\rho)^{5/2}} \quad (5)$$

In the expression, eq 5 and the rest mean end-to-end square distances which follow the prefactor l^2, which causes the mean end-to-end square distances to have dimensions of length^2 is considered for simplicity equal to one and it is omitted. Another interesting mean square end-to-end distance is that of the kth backbone spacer, $\langle r_{bk}{}^2\rangle$ (Figure 2), which is given by:

$$\langle r_{bk}{}^2\rangle = N_b\left(1 + \frac{2}{N_b{}^{3/2}}(u_{bb}D + u_{db}E + u_{dd}F)\right), \quad k = 1, 2, ..., n$$

where

$$D = {}^bS_{1\le i\le k}\times {}^bS_{k+1\le j\le n+1} = \sum_{i=0}^{k-1}\sum_{j=1}^{n-k+1}(i+j)^{-5/2}$$

$$E = {}^bS_{1\le i\le k}\times {}^dS_{k+1\le j\le n+1} + {}^dS_{1\le i\le k}\times {}^dS_{k+1\le j\le n+1}$$
$$= 2\sum_{i=0}^{k-1}\sum_{j=1}^{n-k+1}\sum_{j'=0}^{g}\frac{(f-1)^{j'}}{(i+j+(j'+1)\rho)^{5/2}}$$

$$F = {}^dS_{1\le i\le k}\times {}^dS_{k+1\le j\le n+1}$$
$$= \sum_{i=0}^{k-1}\sum_{j=1}^{n-k+1}\sum_{i'=0}^{g}\sum_{j'=0}^{g}\frac{(f-1)^{i'+j'}}{(i+j+(i'+j'+2)\rho)^{5/2}} \quad (6)$$

Finally the mean square end-to-end distance between the end groups and the grafting point of the kth dendron, Figure 2, is given by

$$\langle R_{dk}{}^2\rangle = N_d\left((g+1) + \frac{2}{N_d{}^{3/2}}(u_{db}G + u_{dd}(H+I))\right),$$
$$k = 1, 2, \ ..., \ n+1$$

where

$$G = {}^bS_{1\le i\le k}\times {}^dS_{j=k} + {}^bS_{k+1\le i\le n+1}\times {}^dS_{j=k}$$
$$= \left(\sum_{i=0}^{k-1} + \sum_{i=1}^{n-k+1}\right)\left(\sum_{j=0}^{g}\frac{(j+1)^2}{((j+1)+i/\rho)^{5/2}} + (f-2)\sum_{j=0}^{g-1}\sum_{j'=0}^{g-1-j}\frac{(f-1)^{j'}(j+1)^2}{((j+j'+2)+i/\rho)^{5/2}}\right)$$

$$H = {}^dS_{i=k}\times {}^dS_{j=k}$$
$$= \sum_{i=0}^{g-1}\sum_{j=0}^{i}(j+1)^{-1/2} + (f-2)$$
$$\left(\sum_{i=0}^{g-2}\sum_{j=0}^{i}\sum_{j'=0}^{i-j} + \sum_{i=0}^{g-1}\sum_{j=0}^{i}\sum_{j'=0}^{g-1-i+j}\right)\frac{(f-1)^{j'}(j+1)^2}{(j+j'+2)^{5/2}} + (f-2)^2\sum_{i=0}^{g-2}\sum_{j=0}^{i}\sum_{i'=0}^{i+1}\sum_{j'=0}^{i-j}\frac{(f-1)^{i'+j'}(j+1)^2}{(j+i'+j'+3)^{5/2}} \quad (7)$$

$$I = {}^dS_{1\le i\le k-1}\times {}^dS_{j=k} + {}^dS_{k+1\le i\le n+1}\times {}^dS_{j=k}$$
$$= \left(\sum_{i=1}^{k-1} + \sum_{i=1}^{n-k+1}\right)\sum_{j=0}^{g}(f-1)^j\left(\sum_{j'=0}^{g}\frac{(j'+1)^2}{((j+j'+2)+i/\rho)^{5/2}} + (f-2)\sum_{j'=0}^{g-1}\sum_{j''=0}^{g-1-j'}\frac{(f-1)^{j''}(j'+1)^2}{((j+j'+j''+3)+i/\rho)^{5/2}}\right)$$

Proper checks for the correctness of eqs 5, 6, and 7 are successful. For example $\langle R_{dk}{}^2\rangle$ reproduces the result of the mean square end-to-end distance between the central core and the end groups of dendritic polymers $\langle R_g{}^2\rangle$, [22] for $N_d = N$, $N_b \to 0$, $u_{dd} = u_{bb} = u_{db} = u$, $n = f_c + 1$ and replacing G of eq 7 with $G/(n+1)$. All three mean square end-to-end distances are used for the study of the behavior of the various parts of the dendronized polymer. The trends of the dependence on the microscopic parameters will be analyzed by means of characteristic graphs based on the expressions eqs 5, 6, and 7.

3. Results and Discussion

In this section we use the three average distances $\langle R_b{}^2\rangle$, $\langle r_{bk}{}^2\rangle$, and $\langle R_{dk}{}^2\rangle$, eqs 5, 6, and 7, in order to analyze the dependence of the conformations of linear dendronized polymers (LDPs) on various microscopic parameters. We analyze the dependence on the "topological" parameters, g, f, n, N_b. and N_d, as well as on the quality of the solvent for both backbone and grafted dendrons and on their compatibility. Characteristic graphs of the points which represent integer values of the parameters g,

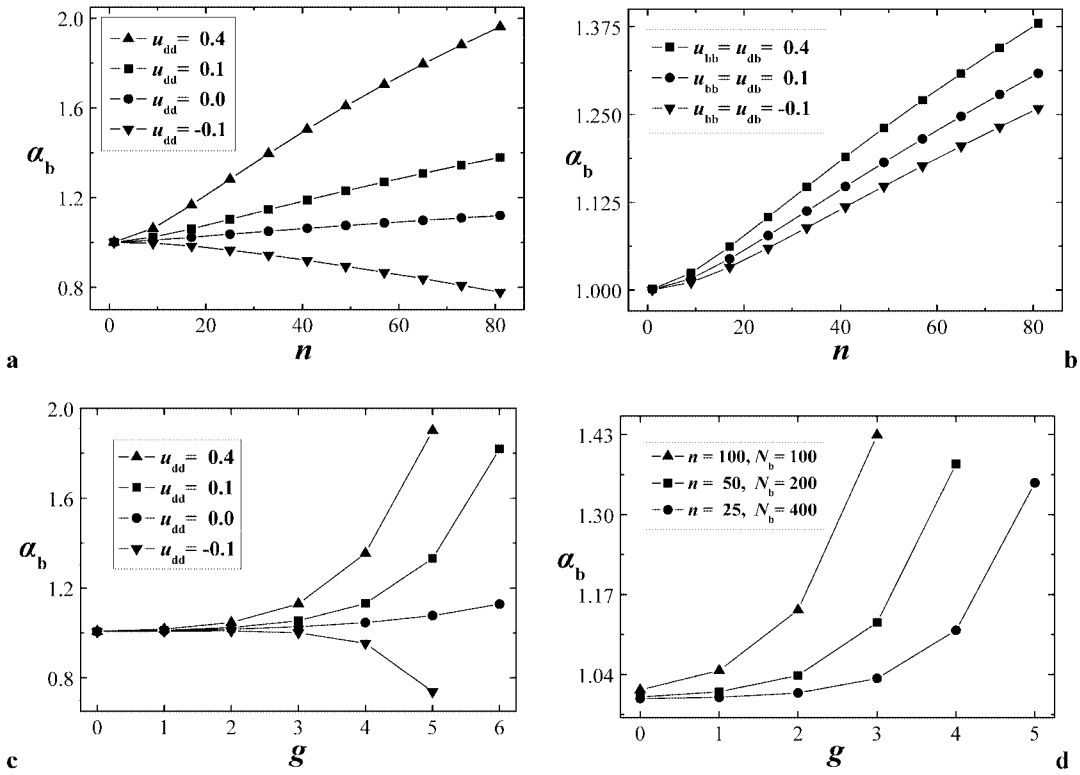

Figure 3. Dependence of the backbone's expansion factor α_b on the number of the backbone segments n and on the dendron's number of generations g for $f = 3$ and $N_d = 100$. (a) $g = 4$, $u_{bb} = u_{db} = 0.4$, $N_b = 100$. (b) $g = 4$, $u_{dd} = 0.1$, $N_b = 100$. (c) $n = 30$, $u_{bb} = u_{db} = 0.4$, $N_b = 100$. (d) $u_{dd} = u_{bb} = u_{db} = 0.4$, $M_b = 10000$. The lines are drawn in order to guide the eye.

f, and n, with joining lines guiding the eye, chosen among many others, are depicted in order to unravel the behavior both of the backbone but also the dendrons of the LDP with emphasis on the effects of the three different kinds of interactions.

3.1. Backbone Properties. The root mean end-to-end square distance of the backbone $\langle R_b^2\rangle^{1/2}$ expresses the average length of the LDPs, while the expansion factor $\alpha_b = \langle R_b^2\rangle^{1/2}/\langle R_b^2\rangle_0^{1/2} = \langle R_b^2\rangle^{1/2}/(n \times N_b)^{1/2}$ measures the effects on the backbone coming from the excluded volume interactions.[24] Selected graphs are presented in Figure 3 in order to exhibit and clarify the behavior of α_b.

In parts a and b of Figure 3, we see how α_b changes on increasing the number of the n backbone segments, each one of length N_b. n which gives also the total number $n + 1$ of the grafted dendrons is proportional to the molecular weight of the backbone $M_b = n \times N_b$. The elongation of the backbone gets larger on increasing the solvent quality of the dendrons with larger values of u_{dd} (Figure 3a). The effects of the u_{dd} interactions on the backbone are shown starting with a comparison with the case of Θ solvent for the dendrons, which are shown in Figure 3a with circles. We see the substantial effects which the u_{dd} interactions between the units of the external dendrons can have on the backbone. Repulsions between the units of the dendrons get them further apart and extend the backbone in a substantial degree in cooperation with the u_{db} and u_{bb} interactions. Attractions though for negative u_{dd} can overcome the rest repulsions and lead as it is shown in Figure 3a to smaller proximities of the dendrons. These force the backbone to shrink and lead to compact structures in agreement with molecular dynamics simulations.[5] The expansion factor α_b becomes also larger for larger values of the u_{bb} and u_{db} interactions (Figure 3b). In Figure 3b we see that the elongation of the backbone is also increasing with u_{bb} and u_{db}. In comparison with Figure 3a, where the LDPs have the same structural parameters, we see though that the solvent quality of the backbone affects only slightly its elongation. No collapse of the backbone does occur in a dendron selective solvent (reverse triangles), with $u_{bb} = u_{db} = -0.1$ but $u_{dd} = 0.1$ positive. This phenomenon is of great scientific and technological interest because it shows that small dendron repulsions is a way to overcome the solubility problem of the otherwise insoluble macromolecules with u_{bb} attractions, like the conjugated polymers[27] or polyamides in various solvents.[28]

In parts c and d of Figure 3, α_b is plotted against g. A first thing to notice is that the small linear-like increase of α_b for small g suddenly becomes essential at certain g depending on the rest parameters, a property which is due to the dendritic character of grafted dendrons. This characteristic behavior of the dendritic polymer structures[22] indicates that the presence of the dendritic side chains becomes more and more significant as g increases, which can be explained by the exponential increase of the interacting units of the dendrons with g and thus by the significant increase of their total excluded volume effects. In Figure 3c, we see the dominant role which the quality of the solvent of the dendrons plays on the conformations of the backbone of the LDP. The value g above which the abrupt increase of interactions and repulsive effects take place depends on the intensity of the u_{dd} interactions. Experimentally evidence of the small increase of the radius of gyration of dendronized poly(*p*-hydroxystyrene)s with g, for relative small values of g, has been given by means of multiangle laser light scattering measurements.[7,16] The sudden increase of the hydrodynamic and viscometric radius of linear-dendritic diblock copolymers after a certain value of g has been confirmed using dynamic light scattering and intrinsic viscometry measurements.[15] Upon moving from the good to the Θ solvent conditions for the dendrons we see that the size of the backbone is reduced, and it finally shrinks in the poor solvent, negative u_{dd}, where the interactions between the units of dendrons become attractive. The total intensity of excluded volume interactions between the

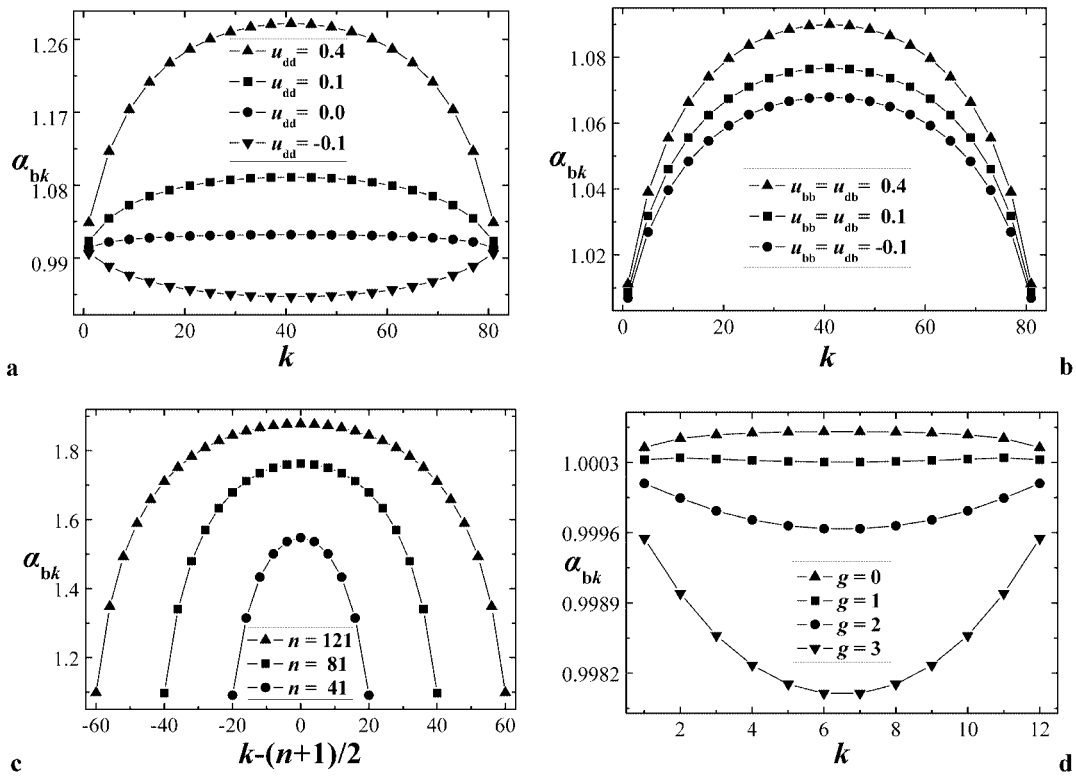

Figure 4. Dependence of the backbone's spacer expansion factor α_{bk} on the position along the backbone k with $N_d = 100$, $N_b = 100$ and $f = 3$. (a) $n = 81$, $g = 5$, $u_{bb} = u_{db} = 0.4$, (b) $n = 81$, $g = 5$, $u_{dd} = 0.1$. (c) $g = 6$, $u_{dd} = u_{bb} = u_{db} = 0.4$. (d) $n = 12$, $u_{bb} = 0.4$, $u_{dd} = u_{db} = -0.1$.

numerous branches of the dendrons affects strongly the size of the backbone, by forcing it to elongate for repulsions and to shrink for attractions between the dendrons. The extension of the LDP's backbone placed in a good solvent on increasing g of the grafted dendrons is in agreement with what has been found by means of Monte Carlo simulations.[12,20] The persistence length of the backbone, which is a measure of its rigidity caused by its stretching, was found to increase with g by using SANS[6] and SEC−MALLS measurements.[16] Experimentally evidence of a compact α-helical to a more extended disordered state transition of a poly(L-lysine) backbone on increasing g has be given both in aqueous solution as well as on a mica surface.[11] Furthermore, by means of the diffusion coefficients measured by NMR spectroscopy and by SANS experiments it has been found that the size of dendronized poly(hydroxy ethylmethacrylate)s[21] and arborescent graft polysterenes,[17] respectively, increases with g and solvent's quality. In Figure 3d finally the influence of the dendron grafting density on the elongation of the backbone is seen, where three LDPs with the same backbone molecular weight $M_b = n \times N_b$ and different numbers of grafted dendrons are plotted. We see that the extension of the backbone is increasing with the grafting density (larger n and constant M_b) of the dendritic side-chains which is caused by the enhanced repulsive interactions between the densely packed and overcrowded dendrons in agreement with previous findings of simulations.[10,20]

In Figure 4 a penetration to the internal structure of the backbone is done, where the k spacer's expansion factor, defined as $\alpha_{bk} = \langle r_{bk}^2\rangle^{1/2}/\langle r_{bk}^2\rangle_0^{1/2} = \langle r_{bk}^2\rangle^{1/2}/N_b^{1/2}$, is plotted versus its position along the backbone k.

In all four families of graphs of Figure 4, we see that α_{bk} shows a symmetrical dependence on the position k along the backbone with the central spacers being more affected than the side ones. In Figure 4a, a comparison between four LDPs with different interactions between the dendrons is done. In good solvent with u_{dd} repulsive the maximum of α_{bk} is obtained in the middle spacers and it decreases by moving to the free ends which is in agreement with previous Monte Carlo simulations.[20] Upon moving from good solvent to Θ solvent conditions for the dendrons, α_{bk} decreases, while in a poor solvent (selective solvent for the backbone) a dominance of the u_{dd} attractions takes place over the rest repulsions and an inverse dependence on α_{bk} is seen. This inversion is more difficult to take place varying the u_{db} and u_{bb} interactions, Figure 4b, showing thus that the u_{dd} are more important than u_{db} and u_{bb} interactions for the affection of the specific parts of the backbone. This is attributed to the large number of intra- and interdendron interactions compared with the corresponding dendron-backbone and backbone-backbone interactions. Increasing the number $n + 1$ of grafting dendrons α_{bk} again shows the same bell-like dependence with larger expansion α_{bk} of the dendrons lying in the middle of the backbone, Figure 4c. Connoly et al.[20] have also found by means of Monte Carlo simulations that the backbone's segments persistence length, which is a measure of their rigidity caused by their stretching, increases with the number of grafted dendrons on the backbone. An interesting observation is that shown in Figure 4d, which shows the dependence of α_{bk} on the number of generations g for negative values of $u_{dd} = u_{db} = -0.1$ and positive repulsion of the units of the backbone. Increasing g and the number of interacting dendron units a reduction of α_{bk} is observed as expected because of the attractions of more units. Beyond the transition from the existence of a maximum to the appearing of a minimum there is a region where two maxima and a minimum can appear because of the simultaneous effects of both repulsive and attractive interactions. We will see more similar behaviors in Figure 5 where the dependence of α_{dk} will be analyzed.

3.2. Dendron Properties. In order to study the behavior of the grafted dendrons we define the expansion factors $\alpha_{dk} = \langle R_{dk}^2\rangle^{1/2}/\langle R_{dk}^2\rangle_0^{1/2} = \langle R_{dk}^2\rangle^{1/2}/N_d^{1/2}$, of the mean square end-to-end distances $\langle R_{dk}^2\rangle$ between the grafting points and the locations

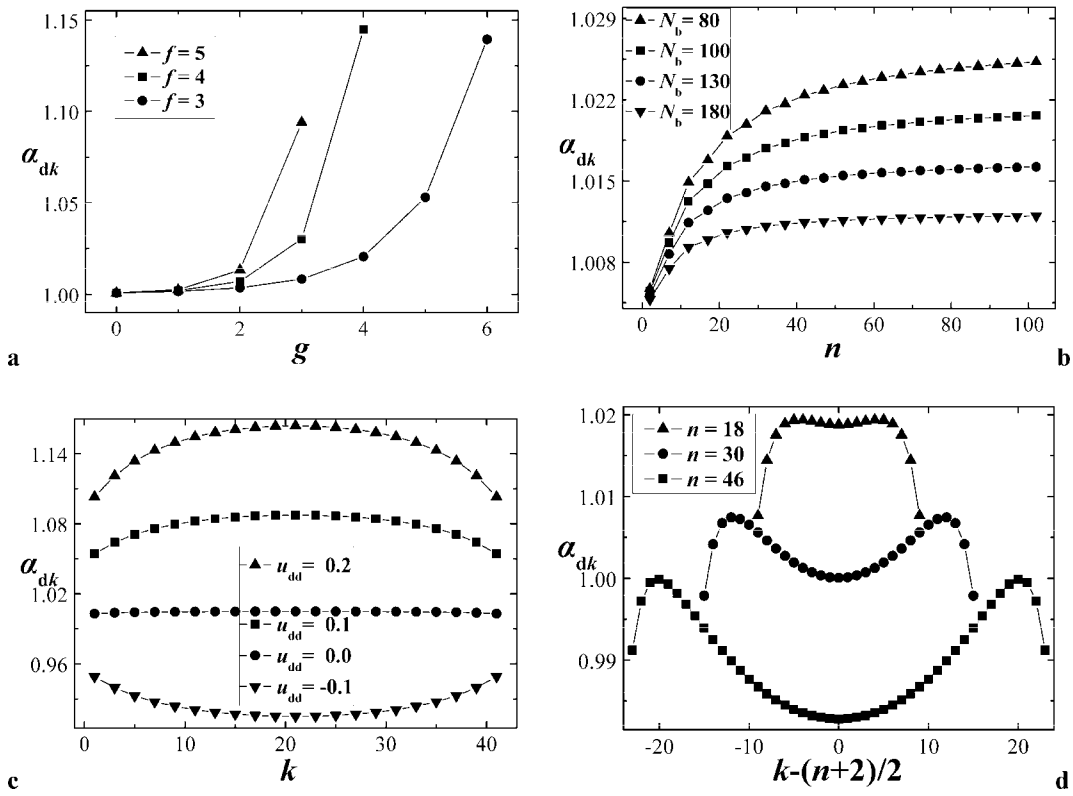

Figure 5. Dependence of the grafted dendron's expansion factor α_{dk} on the dendron's number of generations g, on the number of backbone segments n and on the position along the backbone k. (a) $n = 100$, $k = 51$, $u_{dd} = u_{bb} = u_{db} = 0.4$, $N_d = 100$, $N_b = 100$. (b) $k = (n + 2)/2$, $g = 4$, $f = 3$, $u_{dd} = u_{bb} = u_{db} = 0.4$, $N_d = 100$. (c) $n = 40$, $g = 7$, $f = 3$, $u_{bb} = u_{db} = 0.4$, $N_d = 100$, $N_b = 100$. (d) $g = 7$, $f = 3$, $u_{bb} = 0.2$, $u_{dd} = -0.1$, $u_{db} = 6.68$, $N_d = 50$, $N_b = 50$.

of their end groups. They provide the information whether the dendron's free ends tend to locate near the backbone (small α_{dk}) or out in the free space (large α_{dk}). In parts a and b of Figure 5, we focus on the central dendron ($k = (n + 2)/2$, n even), where the excluded volume phenomena become stronger. Increasing the number g of generations the expansion of the central dendrons increase, Figure 5a, mildly for small g and in an abrupt way for larger g. The transition from the small increase to the large one depends on the rest parameters like in the simple dendrimers. It is shown for example in Figure 5a that larger functionalities f, i.e. larger dendron densities, lead to earlier transitions, which is in agreement with our previous studies on dendritic polymers.[22] The almost linear increase of $<R_{dk}^2>^{1/2}$ with g for LDPs with $f = 3$ (for relative small values of g) has also been reported previously based both on computational[10,19] but also on experimental[18,21] results. The increase of encapsulation properties of LPDs, for applications as unimolecular nanocontainers, has been found experimentally to increase with g,[14] indicating an increase in the overall volume of the cavities. This behavior can be explained by means of Figure 5a, which shows that on increasing g the end groups of the extended dendrons are forced further away from the backbone, and the fact that in the good solvent, $\langle r_{bk}^2\rangle^{1/2}$, i.e. the distance between two successive grafting points along the backbone, increases also with g. A way to reduce the overcrowding of the branches in the region next to the backbone(larger α_{dk}) is to increase the distance N_b between two successive grafting points along the backbone (Figure 5b). This limiting behavior of the dendron's radius of gyration on increasing n, after a certain value of n, has also been observed by P. M. Welch and C. F. Welch.[10] A "picture" of the profiles of some LDPs is given in Figures 5c and 5d, where α_{dk} is plotted against k. In Figure 5c, we see that in the good solvent region the LDP could be described as an elongated cylinder or as a prolated ellipsoid with the perpendicular diameter to decrease by moving from the cylinder's center to the ends, which is in agreement with the findings of Nyström et al.[29] Further increase of the central diameters are observed for larger u_{dd} values. The increase of the LDP's diameter on increasing solvent quality has been also observed experimentally.[21] What we also see in Figure 5c is that a transition to an opposite behavior in the LDP's profile takes place on decreasing solvent quality of the dendrons. Moingeon et al.[30] have suggested that the overcrowding of the dendrons could be absorbed by the relaxing of the dendrons grafted in both extremities of the backbone. This phenomenon is seen in Figure 5c in the case of $u_{dd} > 0$ where α_{dk} for $k = 1$ and $k = n + 1$ is smaller than for the other k's. When the various interactions become antagonizing special features emerge. In Figure 5d we see that by choosing specific structural characteristics and solvent environment for the LDP we can obtain fluctuations in the longitudinal structure opening new possibilities for structures with two symmetrical behaviors at the two half's of the chain. Similar longitudinal instability of the cylindrically uniform structure and appearance of undulations has been reported recently by Polotsky et al. by means of a self-consistent field theory[31] for comb polymers with a very rigid backbone and flexible side-chains in a poor solvent.

3.3. LDP's Shape. In order to characterize the overall shape of the LDPs we define their aspect ratio between their two sizes along and perpendicular to the backbone as $AR = \langle R_b^2\rangle^{1/2}/\langle R_{dk}^2\rangle^{1/2}$, and we focus on the central dendrons with $k = (n + 2)/2$, which are more affected than the side ones (see also Figure 5c). Small and large values of AR means disk-like and cylindrical-like shapes while values around one mean spherical-like LDPs. We examine the behavior of AR on increasing either g or n, which means on increasing the LDP's mass either in the perpendicular direction or in the direction along the backbone. A variety of behaviors of the ratio are depicted in Figure 6 where the general trends can be understood. The initial decrease of the aspect ratio

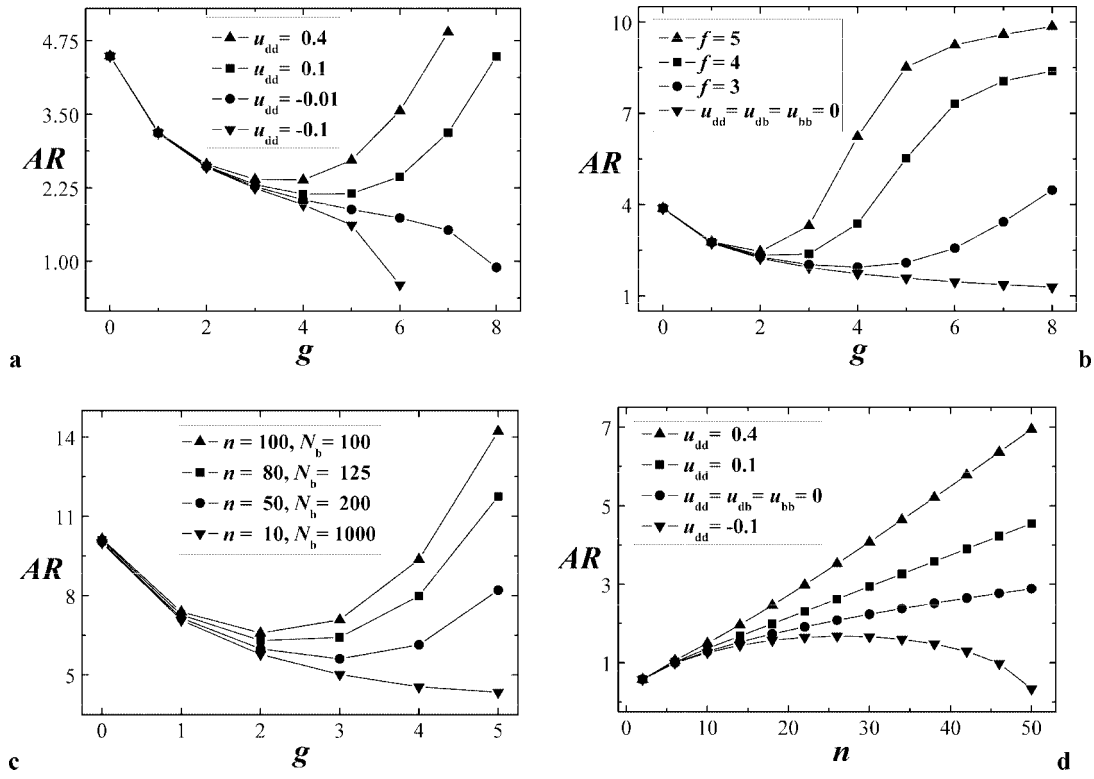

Figure 6. Dependence of the LDPs aspect ratio *AR* on the dendron's number of generations *g* and on the number of backbone segments *n* for $N_d = 100$. (a) $n = 20$, $k = (n + 2)/2$, $f = 3$, $u_{bb} = u_{db} = 0.4$, $N_b = 100$. (b) $n = 15$, $k = (n + 2)/2$, $u_{dd} = u_{bb} = u_{db} = 0.4$, $N_b = 100$. (c) $k = (n + 2)/2$, $f = 3$, $u_{dd} = u_{bb} = u_{db} = 0.4$, $M_b = 10000$. (d) $k = (n + 2)/2$, $g = 5$, $f = 3$, $u_{bb} = u_{db} = 0.4$, $N_b = 100$. The graphs b and d include also the ideal chain with all *u*'s zero.

in the small region of *g* mainly comes from the extension of the dendrons and the increase of $\langle R_{dk}^2\rangle^{1/2}$, Figure 6a. Increasing further *g* when u_{dd} is attractive brings closer the dendrons and decreases the backbone size. This means a decrease of $\langle R_b^2\rangle^{1/2}$ and an abrupt decrease of *AR*. A different behavior happens for u_{dd} positive. Increasing *g* to large values takes away the dendrons, their effects on $\langle R_{dk}^2\rangle^{1/2}$ becomes smaller leaving $\langle R_b^2\rangle^{1/2}$ to their large values which give a large aspect ratio. This is seen by comparing with Figures 3c (triangles) and 5a (circles), which represent both LDPs having the same values of N_b, N_d, *f*, u_{bb}, u_{db}, and u_{dd}. We see that the expansion factor of the backbone is larger and grows faster with *g* than that of the grafted dendrons, despite the fact that *n* is over than three times larger in the latter case. The initial decrease with the final increase of the aspect ratio explains the existence of the minima occurred in Figure 6a for u_{dd} positive. That is, while for small values of *g*, *AR* decreases by the extra addition of macromolecular branches on the dendrons, it increases on further increase of *g*, because α_b increases rapidly and overcomes the growing of the dendrons. Similar minima are observed in Figure 6, parts b and c, where we see that the LDPs in good solvents adopt the cylindrical shape at smaller values of *g* for larger *f* and larger *n* (at fixed M_b), because in both cases the enhanced number of branches force the backbone to elongate much more than the dendrons. No *f* dependence appears when the *u*'s are zero and the chains behave ideally. The LDP's transition from a coil-like to a rod-like form on increasing *g* has also been reported before.[6,7,16] This is also the case for the dendronized part of a diblock copolymer built from a linear and a dendronized polymer.[15] The cylindrical shape of LDPs with high-generation dendrons has been confirmed by means of SANS experiments.[18] On increasing *n* the LDPs assume a cylindrical "1-dimensional" shape, except the case of selective solvent for the backbone where after a critical value of *n* the LDP adopts a disk-like shape with AR smaller than one, Figure 6d. This happens because the number of the attractive grafted dendrons becomes large enough to force the backbone to shrink. The transition of the LDPs shape from a spherical to tubular on increasing *n* in good solvents is in agreement with results of previous findings.[5,9,10] The aspect ratio *AR* which we analyzed in the present section and the properties described in this work is only a part of what the present effort can provide.

Conclusion

Our study of the conformational properties of dendritic homopolymers is extended to linear dendronized polymers (LDPs) made of a backbone and grafted dendrons of different chemical nature. The changeable shape and size of the LDPs makes them very promising to a variety of potential uses. The systematic variation of the quality of the solvent for both the dendrons and the backbone reveal important behaviors which are also affected by the rest "topological" parameters. The expansion factor and the extension of the backbone is strongly depended on the quality of the solvent of the dendrons. It is large in a common good solvent where the backbone is forced to elongate on increasing *g* and the grafting density of the dendrons. It is slightly smaller in a dendron selective solvent while in a backbone selective solvent the attractions between the dendron segments causes the shrinkage of LDP. The backbone spacer's expansion factor shows a symmetrical dependence on the position along the backbone with the central spacers being more affected than the side ones. A similar behavior is observed for the grafted dendrons the extension of which gives a picture of the profile and the perpendicular diameter of the LDP. It decreases or increases by moving from the backbone's center to the ends in a common good or in a backbone selective solvent respectively. By choosing specific structural characteristics and solvent environment we can obtain fluctuations in the longitudinal structure of the LDP. In a good

solvent the LDP can be described as an elongated cylinder or a prolated ellipsoid while the extension of the dendrons is increasing on increasing g, f, and n or on decreasing N_b, with this expansion being much smaller than the corresponding expansion factor of the backbone. The LDP's aspect ratio in a good solvent reveals that its cylindrical geometry is reached at smaller values of g for larger f or grafting densities. In a backbone selective solvent the LPD reduces to a spherical shape and finally after a certain value of g or n shrinks to a disk-like shape.

Acknowledgment. The authors thank Professor G. Floudas for helpful discussions. This research project is cofinanced by the E.U.-European Social Fund (75%) and the Greek Ministry of Development-GSRT (25%) by Grant PENED 03ED856.

References and Notes

(1) (a) Boas, U.; Heegaard, P. M. H. *Chem. Soc. Rev.* **2004**, *33*, 43–63. (b) Gillies, E. R.; Fréchet, J. M. J. *Drug Discov. Today* **2005**, *10*, 35–43. (c) Qui, L. Y.; Bae, Y. H. *Pharm. Res.* **2006**, *23*, 1–30. (d) Guillot-Nieckowski, M.; Eisler, S.; Diederich, F. *New J. Chem.* **2007**, *31*, 1111–1127. (e) Paleos, C. M.; Tsiourvas, D.; Sideratou, Z. *Mol. Pharm* **2007**, *4*, 169–188. (f) Wigglesworth, T. J.; Teixeira, F., Jr.; Axthelm, F.; Eisler, S.; Csaba, N. S.; Merkle, H. P.; Meier, W.; Diederich, F. *Org. Biomol. Chem* **2008**, *6*, 1905–1911.

(2) (a) Helms, B.; Fréchet, J. M. J. *Adv. Synth. Catal.* **2006**, *348*, 1125–1148. (b) Kowalewska, A. *J. Organomet. Chem.* **2008**, *693*, 2193–2199.

(3) (a) Gupta, U.; Agashe, H. B.; Asthana, A.; Jain, N. K. *Biomacromolecules* **2006**, *7*, 649–658. (b) Benhabbour, S. R.; Parrott, M. C.; Gratton, S. E. A.; Adronov, A. *Macromolecules* **2007**, *40*, 5678–5688.

(4) (a) Schlüter, A. D. *Top. Curr. Chem.* **1998**, *197*, 165191. (b) Schlüter, A. D.; Rabe, J. P. *Angew. Chem., Int. Ed.* **2000**, *39*, 864–883. (c) Teertstra, S. J.; Gauthier, M. *Prog. Polym. Sci.* **2004**, *29*, 277–327. (d) Schlüter, A. D. *Top. Curr. Chem.* **2005**, *245*, 151–191. (e) Frauenrath, H. *Prog. Polym. Sci.* **2005**, *30*, 325–384.

(5) Jahromi, S; Coussens, B.; Meijerink, N.; Braam, A. W. M. *J. Am. Chem. Soc.* **1998**, *120*, 9753–9762.

(6) Ouali, N.; Méry, S.; Skoulios, A.; Noirez, L. *Macromolecules* **2000**, *33*, 6185–6193.

(7) Das, J.; Yoshida, M.; Fresco, Z. M.; Choi, T.-L.; Fréchet, J. M. J.; Chakraborty, A. K. *J. Phys. Chem. B* **2005**, *109*, 6535–6543.

(8) Percec, V.; Ahn, C.-H.; Ungar, G.; Yeardley, D. J. P.; Möller, M.; Sheiko, S. S. *Nature* **1998**, *391*, 161–164.

(9) Lübbert, A.; Nguyen, T. Q.; Sun, F.; Sheiko, S. S.; Klok, H.-A. *Macromolecules* **2005**, *38*, 2064–2071.

(10) Welch, P. M.; Welch, C. F. *Nano Lett.* **2006**, *6*, 1922–1927.

(11) Lee, C. C.; Fréchet, J. M. J. *Macromolecules* **2006**, *39*, 476–481.

(12) Christopoulos, D. K.; Terzis, A. F.; Vanakaras, A. G.; Photinos, D. J. *J. Chem. Phys.* **2006**, *125*, 204907.

(13) Namazi, H.; Adeli, M.; Zarnegar, Z.; Jafari, S.; Dadkhah, A.; Shukla, A. *Colloid Polym. Sci.* **2007**, *285*, 1527–1533.

(14) Zhang, *Macromol. Rapid Commun.* **2006**, *27*, 626−630.

(15) Santini, C. M. B.; Hatton, T. A.; Hammond, P. T. *Langmuir* **2006**, *22*, 7487–7498.

(16) Yoshida, M.; Fresco, Z. M.; Ohnishi, S.; Fréchet, J. M. J. *Macromolecules* **2005**, *38*, 334–344.

(17) Choi, S.; Briber, R. M.; Bauer, B. J.; Topp, A.; Gauthier, M.; Tichagwa, L. *Macromolecules* **1999**, *32*, 7879–7886.

(18) Förster, S.; Neubert, I.; Schlüter, A. D.; Lindner, P. *Macromolecules* **1999**, *32*, 4043–4049.

(19) Christopoulos, D. K.; Photinos, D. J.; Stimson, L. M.; Terzis, A. F.; Vanakaras, A. G. *J. Mater. Chem.* **2003**, *13*, 2756–2764.

(20) Connolly, R.; Bellesia, G.; Timoshenko, E. G.; Kuznetsov, Y. A.; Elli, S.; Ganazzoli, F. *Macromolecules* **2005**, *38*, 5288–5299.

(21) Hietala, S.; Nyström, A.; Tenhu, H.; Hult, A. *J. Polym. Sci., Part A: Polym. Chem.* **2006**, *44*, 3674–3683.

(22) Efthymiopoulos, P.; Kosmas, M.; Vlahos, C.; Gergidis, L. N. *Macromolecules* **2007**, *40*, 9164–9173.

(23) (a) Fixman, M. *J. Chem. Phys.* **1955**, *23*, 1656–1659. (b) Edwards, S. F. *Proc. Phys. Soc.* **1965**, *85*, 613–624. (c) Edwards, S. F. *J. Phys. A: Math. Gen* **1975**, *8*, 1171–1177.

(24) Yamakawa, H. *Modern Theory of Polymer Solutions*; Harper and Row: New York, 1971.

(25) (a) Kosmas, M.; Vlahos, C.; Avgeropoulos, A. *J. Chem. Phys.* **2006**, *125*, 094908. (b) Rangou, S.; Theodorakis, P. E.; Gergidis, L. N.; Avgeropoulos, A.; Efthymiopoulos, P.; Smyrnaios, D.; Kosmas, M.; Vlahos, C.; Giannopoulos, Th. *Polymer* **2007**, *48*, 652–663.

(26) (a) Vlahos, C. H.; Kosmas, M. K. *J. Phys. A: Math. Gen.* **1987**, *20*, 1471–1483. (b) Whittington, S. G.; Kosmas, M. K.; Gaunt, D. S. *J. Phys. A: Math. Gen.* **1988**, *21*, 4211–4216. (c) Kosmas, M. K.; Gaunt, D. S.; Whittington, S. G. *J. Phys. A: Math. Gen* **1989**, *22*, 5109–5116.

(27) (a) Li, W.-S.; Jiang, D.-L.; Aida, T. *Angew Chem., Int. Ed.* **2004**, *43*, 2943–2947. (b) Fei, Z.; Han, Y.; Bo, Z. *J. Polym. Sci., Part A: Polym. Chem.* **2008**, *46*, 4030–4037.

(28) Miao, Y.; Wu, G.; Zhou, L.; Xu, W.; Xia, X.; Xu, W. *J. Appl. Polym. Sci.* **2008**, *109*, 397–405.

(29) Nyström, A. M.; Furo, I.; Malmström, E.; Hult, A. *J. Polym. Sci., Part A: Polym. Chem.* **2005**, *43*, 4496–4504.

(30) Moingeon, F.; Roeser, J.; Masson, P.; Arnaud, F.; Méry, S. *Chem. Commun.* **2008**, 1341–1343.

(31) Polotsky, A.; Daoud, M.; Borisov, O.; Charlaganov, M.; Leermakers, F. A. M. *Int. J. Polym. Anal. Charact.* **2007**, *12*, 47–55.

MA801609F